Statistical properties of the eigenfrequency distribution of three-dimensional microwave cavities

S. Deus,[1] P.M. Koch,[1] and L. Sirko[1,2]

[1]*Department of Physics, State University of New York at Stony Brook, Stony Brook, New York 11794-3800*
[2]*Polish Academy of Sciences, Aleja Lotników 32/46, 02-688 Warszawa, Poland*

(Received 22 November 1994)

We measured the transmission spectra of asymmetrically shaped three-dimensional (3D) microwave cavities to determine resonant frequencies. We used the Balian-Bloch formula [R. Balian and C. Bloch, Ann. Phys. (N.Y.) **84**, 559 (1974); **64**, 271 (1971), Eq. (I.1)] for electromagnetic waves in a three-dimensional cavity with smooth walls to check that very few resonances were missed up to 14 GHz. After normalizing them with the local mean eigenmode spacing, we unfolded the resonance spectra and found that the distribution of electromagnetic eigenmodes of the irregular 3D microwave cavities displays a statistical behavior characteristic for classically chaotic quantum systems, viz., the Wigner distribution. We found that this result did not depend on the exact irregular shape of the 3D cavity, suggesting that it is universal.

PACS number(s): 41.20.Bt, 84.40.Cb, 05.45.+b

I. INTRODUCTION

The statistical properties of bounded quantum systems have been intensively investigated theoretically and experimentally [1], especially for those whose classical counterparts have two degrees of freedom, such as planar billards. The correspondence between the eigenvalue statistics of a quantum system and the properties of its classical counterpart was found. When the classical counterpart is integrable, a Poisson distribution (level clustering) of the eigenvalue spacings is expected, whereas for nonintegrable (classically chaotic) counterparts, a Wigner distribution (level repulsion) characteristic of the Gaussian orthogonal ensemble (GOE) is expected.

In random matrix theories, several different Gaussian ensembles were studied [2]. The most important are the GOE, the Gaussian symplectic ensemble (GSE), and the Gaussian unitary ensemble (GUE). The GUE is not invariant under time reversal, but the GOE and the GSE are. Furthermore, the GOE (GSE) corresponds to systems with an integral (a half-integral) total angular momentum measured in units of $\hbar$.

GOE statistics have been found in a number of different physical problems, e.g., in the level spacing distribution of atomic nuclei [3], of higher acoustic eigenfrequencies of small aluminum blocks [4] and of the hydrogen atom in a strong magnetic field, i.e., the so-called diamagnetic Kepler problem [5–7]. Universality in the response of hydrogen energy levels to the magnetic field in the chaotic region was shown in [8]. Quantum phase space behavior for nonhydrogenic atoms in magnetic fields was studied [9]. Relations between the degree of chaos in a classical system and the level spacing statistics of its quantal counterpart are discussed in [1, 10, 11].

Poisson statistics in an atomic physics problem was investigated [12]. The energy-level statistics of the diamagnetic lithium Rydberg spectrum in a regime of regular classical motion showed Poisson-type behavior for the distribution of nearby levels.

Recently, two-dimensional (2D) electromagnetic systems, particularly microwave cavities, have emerged as a laboratory tool for studying some issues in quantum chaos [13–16], by which we mean the properties of a quantal system whose classical counterpart is chaotic. Reaching the latter involves a noncommuting double limit $\hbar \to 0$ and $t \to \infty$ [17]. Some general features of eigenvalue spectra, such as their statistical properties, are reasonably well understood [18]. For these 2D cavities (assumed to be dissipationless), Maxwell's equations and their boundary conditions lead to a Helmholtz equation whose solutions yield eigenfrequencies and eigenfunctions that are equivalent to those for the 2D Schrödinger equation. Because one is able to measure both the frequencies and the field distributions of 2D electromagnetic cavity resonances, this analog system has been exploited for quantum chaos studies [19].

In 3D cavities, the electromagnetic Helmholtz equation and its boundary conditions are not mathematically equivalent to the 3D Schrödinger equation (the wave function is scalar) and its boundary conditions due to the vector nature of the electromagnetic field. Therefore, we do not directly investigate here an electromagnetic analog for quantum systems. However, Balian and Bloch have shown [20, 21] that there is a strong analogy between the 3D Laplace equation and the electromagnetic Helmholtz equation in three dimensions. For example, the leading volume term of the density of the electromagnetic eigenmodes (vector field) is twice that corresponding to a scalar field, e.g., the density of the eigenvalues of the 3D Schrödinger equation. The factor 2 is due to the two orthogonal, transverse polarizations of the electromagnetic field.

Maxwell's equations in the asymptotic limit $\lambda \ll x$, where λ is the wavelength and x the size of a resonant structure, can be solved by and associated with ray propagation (see, e.g., [22]). Thus the discussion of systems associated with regular rays versus systems associated with chaotic rays in this limit is an interesting possibility

for 3D bound electromagnetic systems.

In general, 3D cavities are more generic than 2D cavities in that the ray phase space is globally connected (Arnold's diffusion) for the case of near-integrable systems, whereas in 2D systems resonance layers at separatrices are isolated from each other by Kolmogorov-Arnold-Moser (KAM) surfaces. (See, e.g., [23] for 3D billards, generic systems, Arnold's diffusion, and KAM surfaces.) Quantum dynamics of 3D billards that are stochastic in the classical ray limit was discussed in [24] and applied to a periodically perturbed waveguide.

In this paper we present an experiment studying the statistical properties of the electromagnetic eigenmodes of 3D cavities. The question motivating this work is simple: Do we get the same statistical results as in 2D cavities, viz., Poisson statistics for regularly shaped cavities and GOE statistics for irregularly shaped cavities? (See Sec. III C 2 for the definition of Poisson and GOE statistics and Sec. II for the definition of irregularly shaped cavities.) The answer turns out to be yes. Therefore, we infer that a relation between solutions of the 3D Helmholtz equation and those of the 3D Schrödinger equation (each with appropriate boundary conditions) exists.

The electromagnetic eigenmodes for regularly shaped 3D cavities, e.g., parallelepiped, sphere, cylinder, ellipsoid of revolution, etc., can be easily calculated since the Helmholtz equation with this kind of boundary conditions is separable and therefore exactly solvable. An example for such a calculation with its result for the nearest-neighbor spacing distribution, which is indeed Poisson-like, is shown in the Appendix. Therefore, an experimental approach is particularly useful for irregularly shaped cavities for which numerical solutions are extremely difficult to obtain. Sophisticated software packages such as MAFIA [25] could, in principle, allow the calculation of the electromagnetic eigenmodes of 3D cavities of any shape, but we estimate that the required number of mesh points needed to specify accurately the irregular boundary surfaces that interest us here would lead to calculations requiring such an immense amount of CPU time to get a reasonable number of eigenvalues with a reasonable accuracy that this method does not now seem to be a feasible alternative to the experiment. This may change as available computers become even more powerful.

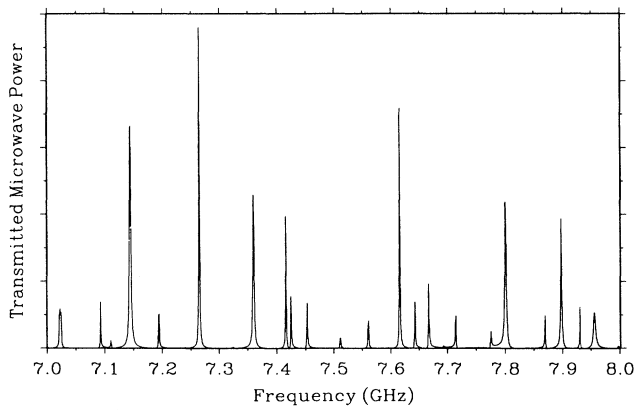

FIG. 1. Transmitted microwave power in the frequency range between 7 and 8 GHz. Looking carefully, one can identify 24 cavity resonances in this frequency range. If we apply a logarithmic y scale (see Fig. 2), we can identify four more resonances with relative amplitudes that are too small to show up on a linear y scale.

II. EXPERIMENT

In the experiments we used different irregularly shaped microwave cavities. By irregular we mean that the cavity has no symmetry of rotation or reflection. Of course, any real "symmetrical" cavity has manufacturing imperfections (not to mention openings for antennas or irises that couple power in or out) that break its symmetry, but these are usually neglected as long as they are much smaller than the wavelength. We made our irregular 3D cavities by soldering together the edges of thin sheets of brass "shim stock."

We measured cavity spectra using a transmission method because we found it to lead to a more precise identification of eigenmodes than the reflection method. This superiority is substantial because sharp peaks emerging from a negligible background are observed and not dips in a constantly varying reflected power level. Specifically, we used a Gigatronics Model 910/2-18 microwave synthesizer together with a Hewlett Packard Model HP8484A power sensor and Model HP436A power meter to measure the transmitted power. The frequency could be varied in 1-MHz steps between 2 and 18.5 GHz. The microwaves were transmitted to the resonator through a low-loss microwave cable. Coupling to the field inside the cavity was accomplished by small elec-

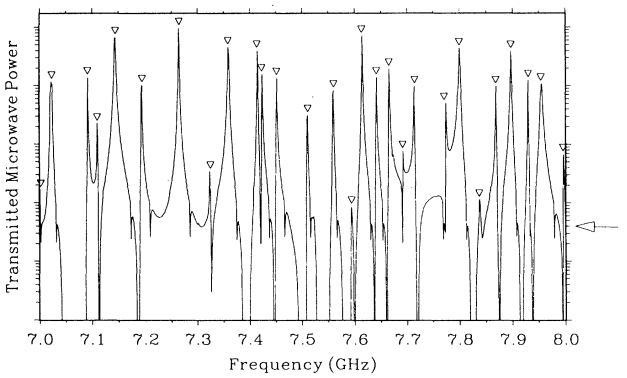

FIG. 2. Figure 1 with logarithmic power axis. We identify 28 resonances (marked by inverse triangles). The subjective, qualitative selection criterion was a distinctive peak structure. Peaks from dispersion shape lines, e.g., at 7.323 GHz, 7.692 GHz, and 7.772 GHz, were taken into consideration. The small shoulder peaks that frequently show up at the power level near the arrow at the right-hand vertical axis are spurious and should be ignored. They were produced by the power meter changing from a less sensitive to a more sensitive range.

tric dipole antennas made of copper wire. The length of each antenna was approximately 2 mm, long enough to get a satisfactory coupling over the whole frequency range but short enough to make only a small perturbation.

The microwave power transmitted through the cavity was measured as a function of frequency under computer control, using the IEEE-488 general purpose interface bus. Each transmission spectrum was stored on disk for later graphical examination on the computer screen. The resonance frequencies are easily identified from such transmission spectra (see Figs. 1 and 2) up to the limit of approximately 14 GHz.

The resonator quality Q is defined as $Q = \nu/\Delta\nu$, where ν is a typical eigenfrequency and $\Delta\nu$ its width. As is well known for regular cavities, the resonator Q is mode-number dependent, but qualitatively one can speak of a typical, "average" Q. In general, $\Delta\nu$ increases as ν increases; this, plus the quadratic increase [see Eq. (1)] of eigenfrequency density with frequency, always makes it difficult to resolve resonances above some critical frequency (see Fig. 3). The resonator quality Q depends on the surface conductivity of the cavity material and on the volume of the cavity. The cavities we used had a volume near 500 cm^3 and a typical Q near 2000.

Two successive eigenfrequencies can just be resolved if they are separated by at least their typical width $\Delta\nu$ and have comparable amplitudes. Thus a higher resonator quality Q allows measurements at higher frequencies, where the density of the resonances increases rapidly. This yields a higher total number of resonances and thus more reliable statistics. On the other hand, higher Q values require a smaller step width of the frequency scanning, which is more time consuming. We decided to measure with a step width of 1 MHz. Our upper frequency limit had to shrink to 14 GHz to make sure that not too many resonances were missed. In this frequency range, we identified 466 eigenfrequencies, which led to reasonable statistics. To do so, however, we found it important to compare spectra obtained by using multiple coupling locations [4] in order to ensure that an accidental occurrence of eigenfunction nodes at a particular location did not lead to missed levels. Our experience is that three widely spaced coupling locations are sufficient for irregularly shaped 3D cavities. If an eigenfunction has a node at one of the three antennas, it will still be detected by a transmission measurement using the other two antennas. A level will be missed only if two of the nodes of a particular eigenfunction coincide with two of the coupling antennas since then all three possible transmission measurements between the three antennas are blocked. The probability for this case to happen is the square of the probability that one particular antenna will coincide with a node. Therefore, the probability of missing a level due to the occurrence of nodes using three coupling antennas is the square of the probability of losing a level using two antennas. A comparison of our two-antenna and three-antenna measurements shows that approximately one in 20 resonances is lost by using two coupling antennas. Therefore, we estimate that only one resonance in approximately $(20)^2 = 400$ would be lost due to the position of nodes by using three coupling antennas.

A more difficult problem is the possibility of missing eigenfrequencies due to near degeneracy, i.e., missing very small spacings actually present in the eigenfrequency spacing distribution [15]. For example, looking at the leftmost resonance in Fig. 1, one is tempted to ask whether there are two eigenfrequencies under this bump. A comparison of fits to the data using either one or two Lorentzians does not give us a clear answer. Although χ^2 per degree of freedom ($\equiv \frac{\chi^2}{\mathcal{D}}$) for a two-Lorentzian fit to 16 data points is five times as large as for a one-Lorentzian fit, we cannot rule out that this peak is composed of two resonances. There is the possibility that an eigenfrequency, and therefore a small spacing, was missed here (cf. the discussion at the end of Sec. III C 3).

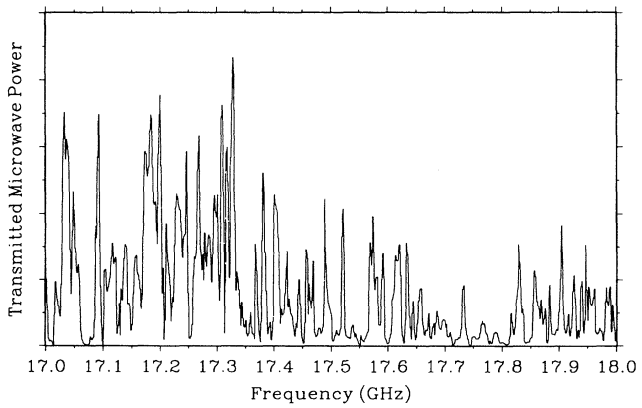

FIG. 3. Transmitted microwave power in the frequency range between 17 and 18 GHz. Many of the resonances cannot be determined since the eigenvalue density has become too high for the quality factor of our cavity.

III. RESULTS

A. Specification of the cavity

Because we found the statistical properties of the ten irregularly shaped cavities we investigated [26] to be similar (i.e., the cavities show similar, Wigner-like (see Sec. III C 2) eigenfrequency spacing distributions and in particular level repulsion), only data obtained with one particular irregular cavity will be presented. The properties of this particular cavity are volume $V = (580 \pm 3)$ cm^3 surface area $A = (414 \pm 6)$ cm^2.

We fabricated this cavity by soldering together plane brass sheets that we deformed by hand before and during the soldering process. We measured accurately the surface area of each originally plane piece, but we must give an uncertainty of ± 6 cm^2 in the surface area due to the uncertainty of ± 1 mm in all soldering joints. We determined the volume of the cavity by measuring the volume of water that it could hold.

Being irregular, the exact shape of this particular cavity is difficult to describe. It was soldered together out of two plane brass sheets, which are shown in Fig. 4. A photograph of the cavity is shown in Fig. 5. The cavity

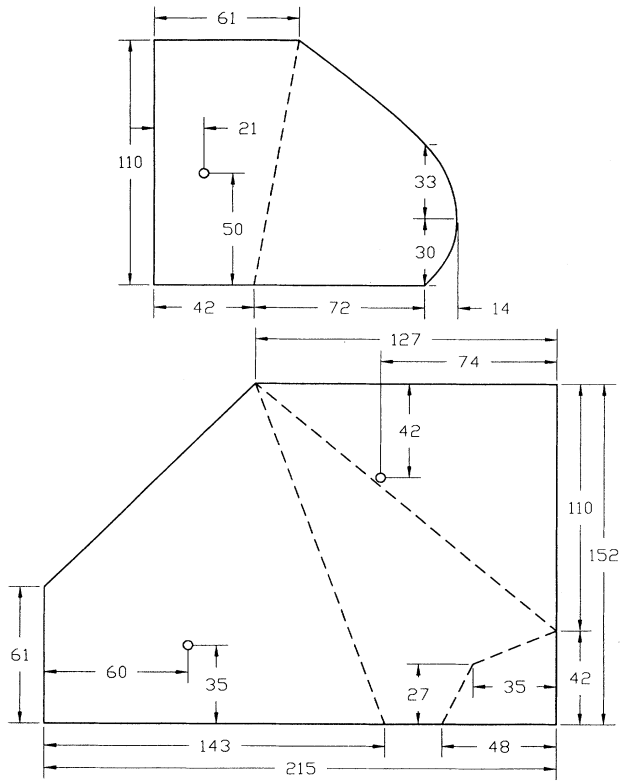

FIG. 4. Scale drawings of the two plane brass sheets out of which the cavity was soldered together. Edges with the same size were joined together. The circles represent the positions of the coupling sites, the dashed lines show the edges.

FIG. 5. Photograph of the cavity.

has five surface segments that may be approximated by surfaces of constant curvature. We estimate the surface curvature term $\frac{2}{3}\int_S \frac{d\sigma_\omega}{R_\omega}$ occurring in the Balian-Bloch formula (see Sec. III B) to be (0.9 ± 0.3) m. We obtained this estimate by measuring the areas σ_i of the surface sections of approximately constant curvature and dividing them by their estimated curvature radii R_i.

B. Check of the Balian-Bloch formula in three dimensions

Balian and Bloch [20] treated theoretically the distribution of electromagnetic eigenmodes in a cavity with perfectly conducting smooth walls. They found the following expression for the density of eigenmodes $\rho_0^{\mathrm{EM}}(k)$ as a function of the wave number k:

$$\rho_0^{\mathrm{EM}}(k) = \frac{1}{\pi^2}\left[Vk^2 - \frac{2}{3}\int_S \frac{d\sigma_\omega}{R_\omega} + \cdots\right], \qquad (1)$$

where V is the volume of the cavity and $\int_S \frac{d\sigma_\omega}{R_\omega}$ is the surface curvature averaged over the whole surface of the cavity. $\rho_0^{\mathrm{EM}}(k)dk$ is the number of modes with wave number between k and $k + dk$.

We compared the cumulative number of eigenfrequencies or the integrated eigenfrequency density $N(\nu)$ of the experimentally determined eigenfrequency distribution (also called the "staircase function," which increases by one at each cavity resonance) with a theoretical result obtained by integrating Eq. (1), now written as a function of the microwave frequency ν:

$$N(\nu) = \frac{8\pi}{3}\frac{V}{c^3}\nu^3 - \frac{4}{3\pi}\frac{1}{c}\int_S \frac{d\sigma_\omega}{R_\omega}\nu + \mathrm{const}, \qquad (2)$$

where c is the speed of light. Only allowing the integration constant to vary, we fitted the integrated Balian-Bloch formula (2) to the experimentally determined staircase function.

For the cavity described in Sec. III A, the agreement with (2) was very good. Figure 6 shows this by comparing the fitted curve (with and without the curvature term) to the experimental staircase for the first 466 eigenfrequencies, which corresponds to the frequency range from 2 to 14 GHz.

In order to check further the agreement with the Balian-Bloch formula (1), we fitted the function

$$N(\nu) = A\nu^3 + B\nu + C$$

to our experimentally obtained staircase function, allowing A, B, and C to vary simultaneously. The obtained fitting parameters A and B lie within the standard deviations of the coefficients of the integrated Balian-Bloch formula (2), $\frac{8\pi}{3}\frac{V}{c^3}$ and $-\frac{4}{3\pi}\frac{1}{c}\int_S \frac{d\sigma_\omega}{R_\omega}$, respectively, while the fitting parameter C lies within the standard deviation of const determined by the one-parameter fit of (2)

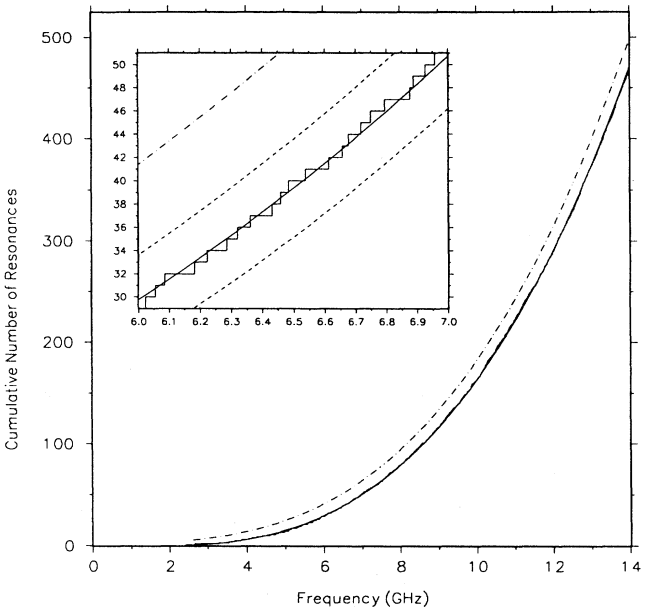

FIG. 6. Comparison of the experimentally obtained staircase function with the theoretical Balian-Bloch formula (2) (solid line). The dash-dotted-line shows the Balian-Bloch prediction with the curvature term omitted, but with the same integration constant used as for the solid line. The dashed lines in the enlarged section of the picture represent the error bars resulting from measurement errors of the volume and the mean surface curvature of the cavity.

to the experimentally obtained staircase function.

Can we infer from the excellent agreement in Fig. 6 that we missed no eigenmodes? No, because a few small fluctuations in the spectrum could have been misinterpreted as eigenmodes, making up for missed eigenmodes. As Sec. III C 3 explains, however, the probability for this to occur is small enough for our purposes.

C. Nearest-neighbor spacing distribution

We used the eigenmode spectra to analyze the nearest-neighbor spacings for short-range correlations. Such a statistical analysis is meaningful only if the spectrum is almost complete, i.e., few eigenfrequencies are missing. The missing of randomly chosen eigenfrequencies of a Wigner distributed spectrum or of a Brody distributed spectrum (Sec. III C 2, below) will yield a distribution with a smaller level repulsion parameter β. In the extreme case of missing randomly the majority of the eigenfrequencies, a Poisson-like distribution will be obtained giving wrong statistical information about the original spectrum. Considering the results shown in Sec. III B, there is a good reason to assume that the spectrum is almost complete and therefore the following analysis is meaningful.

1. Unfolding procedure

We obtained the nearest-neighbor spacing distribution by applying the standard unfolding procedure. From the experimentally determined sequence of frequency eigenvalues $\{\nu_0, \nu_1, \nu_2, \ldots\}$, by taking the differences of the nearest-neighbor eigenfrequencies and normalizing them by the locally averaged eigenmode spacing $\bar{s} = \langle \nu_{i+1} - \nu_i \rangle$, where $\langle\ \rangle$ stands for the *local* average in the frequency range, we obtained the scaled spacings. To get the local average, we divided the spacings by the eigenfrequency density function, which was obtained in two different ways (see Sec. III C 3). We sorted the scaled spacings $s_i := (\nu_{i+1} - \nu_i)/\bar{s}$ so obtained according to their size. After normalizing with the total number of measured eigenmode spacings, we obtained the probability distribution $P(s)$.

2. Brody fit

We fitted the nearest-neighbor spacing distribution to the Brody formula [27, 28]

$$P_\beta^{\text{Brody}}(s) = a s^\beta \exp(-b s^{\beta+1}), \tag{3}$$

$$a = (\beta+1)b,\ b = \{\Gamma(\tfrac{\beta+2}{\beta+1})\}^{\beta+1}, \tag{4}$$

where s is the level spacing normalized by its local average as explained in Sec. III C 1 and β is the so-called level repulsion parameter. The Brody distribution with a level repulsion parameter $\beta = 0$ becomes a Poisson distribution

$$P^{\text{Poisson}}(s) = \exp(-s), \tag{5}$$

which we would expect for classically integrable quantum systems [29, 30]. The distribution (5) describes the statistics of random numbers having no correlation. Therefore, it would represent the levels of a typical regular system.

Taking Eq. (3) with a repulsion parameter $\beta = 1$, we get a Wigner distribution

$$P^{\text{Wigner}}(s) = \frac{\pi}{2} s \exp\left(-\frac{\pi}{4} s^2\right), \tag{6}$$

which we would expect for classically chaotic, integral-spin quantum systems having time-reversal symmetry (GOE) [2].

The level spacing distribution for classically chaotic quantum systems shows a behavior exhibiting level repulsion, i.e., $P(s \to 0) \to 0$. The Wigner distribution gives linear repulsion for small spacings: $P(s) \sim s^\beta$ with $\beta = 1$. Studies of various chaotic systems [30–35] have shown that their level statistics can be those of ensembles of random matrices [2, 36]. For chaotic systems possessing time reversal symmetry, the GOE is applicable [28]. It consists of symmetric matrices built of random Gaussian numbers with zero mean and the variance inversely proportional to the matrix size N. For the limit $N \to \infty$, the GOE level spacing distribution can be approximated well by the Wigner distribution (6) [37, 38].

Although the Brody distribution (3) has no profound physical justification [39], it gives a statistically signifi-

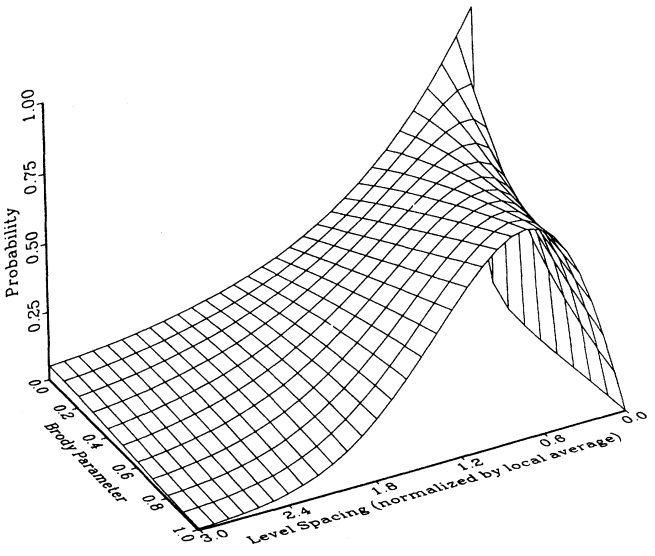

FIG. 7. Brody distribution displayed for the level repulsion parameter β from 0 to 1.

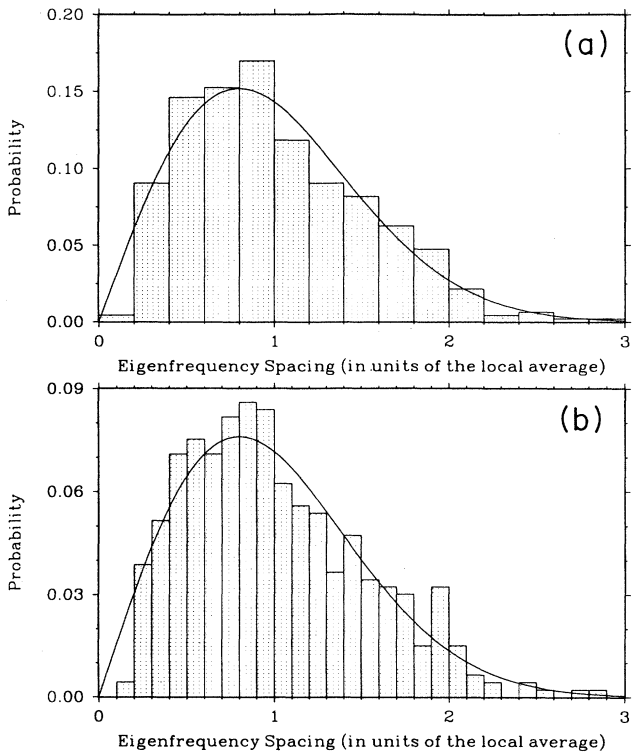

FIG. 8. Eigenfrequency spacing distribution in which the Balian-Bloch density function was used for unfolding the spectrum (method I). The best Brody fit, which is displayed as a solid line, is the Wigner distribution ($\beta = 1.01 \pm 0.06$). Frames (a) and (b) are, respectively, for five and ten intervals per unit average spacing.

cant fit for many practical examples. When the level repulsion parameter β of the unfolded spectrum of a given system is between zero and one, this is usually taken to be an indicator that the corresponding classical system evolves in a mixed phase space of coexisting regular and irregular (chaotic) regions. The Brody distribution furnishes a smooth transition between the Poissonian and Wigner distributions as β varies between zero and one (see Fig. 7).

How can we apply all this to our 3D microwave cavities? Since time reversal symmetry holds for the electromagnetic field inside our irregularly shaped cavities, GOE statistics should be applicable. Therefore, we strongly expect a Wigner level spacing distribution. For a cavity possessing properties of even weak symmetry, level degeneracies will cause departures from this.

3. *Experimentally obtained eigenfrequency spacing distributions*

We obtained the density function applied in the unfolding procedure in two different ways: In method I we used the Balian-Bloch formula for the density function $\rho_0^{\mathrm{EM}}(k)$ [see Eq. (1)] with the measured values of the volume [$V = (580 \pm 3)$ cm^3] and mean curvature [$\int_S \frac{d\sigma_\omega}{R_\omega} = \frac{3}{2}(0.9 \pm 0.3)$ m] and in method II we fitted a polynomial of degree 10 to the experimental curve in Fig. 6, i.e., the cumulative number of resonances, and used the first derivative of this polynomial as the density function. The unfolding procedure II is totally independent of the Balian-Bloch formula (1) and therefore serves us as an additional consistency check of our results.

The level spacing distributions obtained with the two methods are nearly identical; see Figs. 8 and 9, which we obtained as follows. We fitted the Brody function (3) to each respective eigenfrequency spacing distribution. As a consistency check, we did two fits for each unfolding procedure; we divided the unit eigenfrequency spacings into five and ten intervals, respectively. The standard deviation of each column height in the eigenfrequency spacing distributions is the square root of the number of counts represented by the respective column since we have here a counting process and therefore the height of a column (i.e., the number of counts) is Poisson distributed. Fitting with these standard deviations yields, however, a fit that does not represent the data well. We obtained a better fit by applying a constant standard deviation for each column, i.e., Gaussian statistics. For histograms with five columns per unit spacing, we applied a standard deviation of five counts per column, and for histograms with ten columns per unit spacing, we applied a standard deviation of three counts. The used constant standard deviations for each column in the fitting procedure result from the ± 1-MHz error in the determination of a clearly visible eigenfrequency of the cavity that comes from the discrete frequency step used in the experiment. Therefore, the error of a spacing is ± 2 MHz. Unfolding the spectrum with these uncertainties in the eigenfrequency spacings leads to the applied uncertainty in the number of spacings per column in the eigenfrequency distribution function. Additional systematic errors arise because some eigenfrequencies might have been missed or because

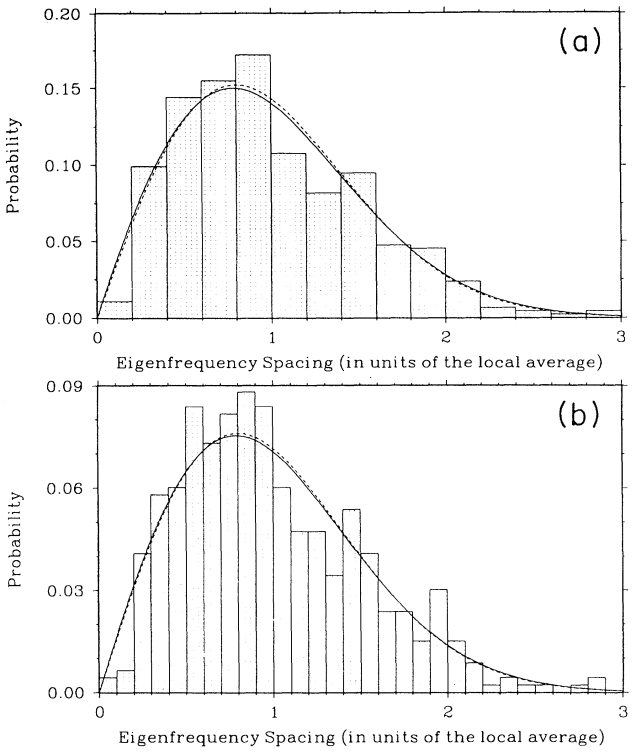

FIG. 9. Eigenfrequency spacing distribution in which a polynomial fitted to the experimental cumulative number of resonances as a function of the frequency was used for unfolding the spectrum (method II). The best Brody fit was given for $\beta = 0.97 \pm 0.06$ (solid line), which is very close to the Wigner distribution (dashed line). Frames (a) and (b) are, respectively, for five and ten intervals per unit average spacing.

some small fluctuations in the transmitted power might have been interpreted as eigenfrequencies. Although we regard the influence of the systematic errors as small because we compared transmission spectra obtained with three different coupling sites, we can neither exclude nor quantify them precisely. However, it is obvious that the systematic error caused by missed eigenfrequencies will be largest for near degeneracies. This is confirmed by a look at the eigenfrequency distribution functions. Figures 8 and 9 clearly show for small spacings a discrepancy between the unfolded experimental distributions and the Brody fits, which are basically Wigner distributions; the experimental results are systematically low here.

The fitted level repulsion parameters are as follows. For unfolding procedure I, five columns per unit mean spacing, $\beta = 1.02 \pm 0.07$, $\frac{\chi^2}{\mathcal{D}} = 0.88$, $\mathcal{D} = 24$; ten columns per unit mean spacing, $\beta = 1.01 \pm 0.06$, $\frac{\chi^2}{\mathcal{D}} = 0.77$, $\mathcal{D} = 49$. For unfolding procedure II, five columns per unit mean spacing, $\beta = 0.96 \pm 0.07$, $\frac{\chi^2}{\mathcal{D}} = 1.14$, $\mathcal{D} = 25$; ten columns per unit mean spacing, $\beta = 0.97 \pm 0.06$, $\frac{\chi^2}{\mathcal{D}} = 1.05$, $\mathcal{D} = 50$.

We believe that method I is more reliable since it uses the Balian-Bloch formula (1) for the density of eigenmodes $\rho_0^{\mathrm{EM}}(k)$, which is obviously experimentally verified (see Fig. 6 and the results of the third-order fit discussed at the end of Sec. III B). As motivated at the beginning of this section, method II is just a consistency check. A polynomial fit can always have small wiggles that do not truly represent the basic mean average. Therefore, we should take the level repulsion parameter $\beta = 1.01 \pm 0.06$ as the final result for the irregularly shaped 3D cavity shown in Figs. 4 and 5. Because missed eigenfrequencies were a more serious problem for the other nine cavities [26] we investigated, we did not obtain quantitatively accurate results for them. Qualitatively, the results were similar.

We investigated how well the nearest-neighbor spacing distribution characteristic for the GUE fits our experimentally obtained data and got a $\frac{\chi^2}{\mathcal{D}}$ 3.6 times as high as for the Wigner (GOE) distribution.

The question arises what influence the fact that some small spacings were missed might have on the level repulsion parameter β. Most of the missed eigenfrequencies were missed because of near degeneracy. If an almost degenerate eigenfrequency is missed, it will show up in the eigenfrequency spacing distribution as a deficit in column(s) for small spacings. The adjacent spacings, however, will not be altered much since the missed spacings are so small.

We investigated what influence the random deletion of some eigenfrequencies of a Wigner-distributed spectrum has on the fitted level repulsion parameter β. We found that β decreases monotonically with an increasing number of randomly deleted eigenfrequencies and approaches zero, i.e., the Poisson distribution, if about 90% of the data points are deleted. β already decreases considerably if a fraction of 30% of the data points is deleted. There is never an increase of β connected with the deletion of data points. Since we found that a Wigner distribution (i.e., $\beta = 1$) fits our experimental spectrum well, we may conclude that missed eigenfrequencies were not a serious experimental problem.

D. Spectral rigidity

The $\bar{\Delta}_3(L)$ statistic of Dyson and Mehta [40], also known as the spectral rigidity, is used extensively in the literature [13, 16, 41–44] to study long-range correlations of energy spectra. The $\bar{\Delta}_3(L)$ statistic measures the spectral average of the stiffness of the spectrum and is defined by

$$\Delta_3(\alpha, L) = \frac{1}{L} \min_{A,B} \int_{\alpha}^{\alpha+L} [N(x) - (Ax - B)]^2 dx, \quad (7)$$

$$\bar{\Delta}_3(L) = \langle \Delta_3(\alpha, L) \rangle_{\alpha}, \quad (8)$$

where $N(x)$ is the cumulative number of eigenfrequencies, i.e., the staircase function jumping by one at each resonance, which is normalized by the local mean eigenfrequency spacing (see Sec. III C 1), and L is the mean eigenfrequency spacing. The minimalization is over the parameters A and B, i.e., $Ax - B$ represents the best fitted straight line to $N(x)$ for $\alpha \leq x \leq \alpha + L$.

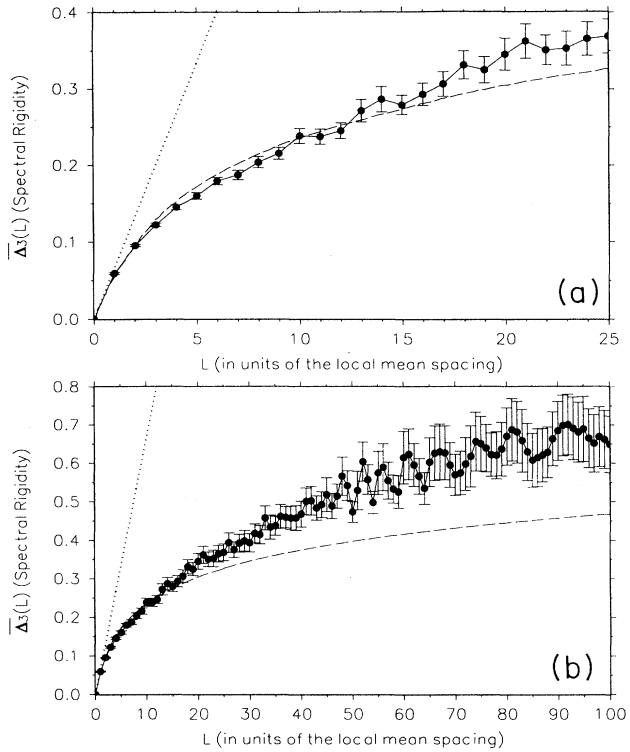

FIG. 10. Spectral rigidity for the irregularly shaped cavity shown in Figs. 4 and 5. The dashed line is a theoretical GOE prediction, whereas the dotted line is $\bar{\Delta}_3(L)$ for the Poisson case.

For an eigenfrequency distribution following Poisson statistics, we would expect a straight line for the spectral rigidity [40]

$$\bar{\Delta}_3^{\text{Poisson}}(L) = \frac{L}{15}, \tag{9}$$

whereas for an eigenfrequency distribution following GOE statistics, we would expect a curve for which there is no analytical form but which may be asymptotically described for large L by [40]

$$\bar{\Delta}_3^{\text{GOE}}(L) \approx \frac{1}{\pi^2}\left[\ln(2\pi L) + \gamma - \frac{\pi^2}{8} - \frac{5}{4}\right]$$

$$= \frac{1}{\pi^2}\ln L - 0.006\,95\ldots, \tag{10}$$

where γ is the Euler constant ($\gamma = 0.577\ldots$).

The spectral rigidity for our cavity is shown in Fig. 10. In the range $0 \leq L \leq 20$, the $\bar{\Delta}_3(L)$ statistic agrees very well with the GOE prediction, for larger L values $\bar{\Delta}_3(L)$ lies slightly above the theoretical GOE curve. This means that up to about 20 adjacent eigenfrequencies are correlated according to the GOE prediction, whereas the correlation of more than 20 eigenfrequencies deviates more significantly from this prediction.

IV. CONCLUSIONS

The nearest-neighbor spacing distribution for the eigenmodes of the investigated 3D cavities clearly shows level repulsion characteristic for classically chaotic quantum systems and is in good agreement with the Wigner surmise (6) [2]. If we had a 2D cavity and therefore a corresponding quantum mechanical system in the classical limit, we could see that almost all trajectories had to be chaotic. (With "almost all" we mean here that the nonchaotic trajectories would be of measure zero.) Therefore, the corresponding quantum mechanical system would have to be ergodic in the classical limit and we would have expected this from the irregular shape of the 2D cavity.

From our spectra obtained with 3D cavities we cannot draw this kind of conclusion. It is interesting, however, to note that 3D cavities seem to be governed by the same statistics as 2D cavities and follow the same "hidden" statistical laws, which are determined by the particular shape of the cavity. There are really clear relations between the type of the system (whether it is "chaotic" or not) and its intrinsic statistical laws, whether or not the system has a quantum mechanical counterpart.

ACKNOWLEDGMENTS

Partial support of this work was supplied by the NSF and by the Fulbright Commission in Germany. We would like to thank J. Verbaarschot, N. Balazs, and R. Blümel for discussions, suggestions, and valuable help.

APPENDIX A: LEVEL SPACING DISTRIBUTION FOR A REGULAR CAVITY

We calculated the first 46 959 eigenfrequencies (which correspond to a frequency range from 0 to 121 GHz) of a cylindrical cavity (radius $R = 3.4722$ cm and height $d = 4.5009$ cm) made of an ideal conductor and filled with vacuum. The TM and TE resonance frequencies of this cavity are given by

$$\nu_{mnp}^{\text{TM}} = \frac{c}{2\pi}\sqrt{\frac{x_{mn}^2}{R^2} + \frac{p^2\pi^2}{d^2}},$$

$$m, p = 0, 1, 2, \ldots, \quad n = 1, 2, 3, \ldots$$

$$\nu_{mnp}^{\text{TE}} = \frac{c}{2\pi}\sqrt{\frac{x_{mn}'^2}{R^2} + \frac{p^2\pi^2}{d^2}},$$

$$m = 0, 1, 2, \ldots, \quad n, p = 1, 2, 3, \ldots,$$

where c is the speed of light, x_{mn} is the nth root of the mth Bessel function $J_m(x)$, and x'_{mn} is the nth root of the first derivative of the mth Bessel function $J'_m(x)$. Since the wave functions for both TM and TE modes contain the factor $\exp(\pm im\phi)$, where ϕ is the angle coordinate in the cylindrical system (ρ, ϕ, z), all eigenvalues except those labeled with $m = 0$ are twofold degenerate. There is an additional degeneracy between TM and TE

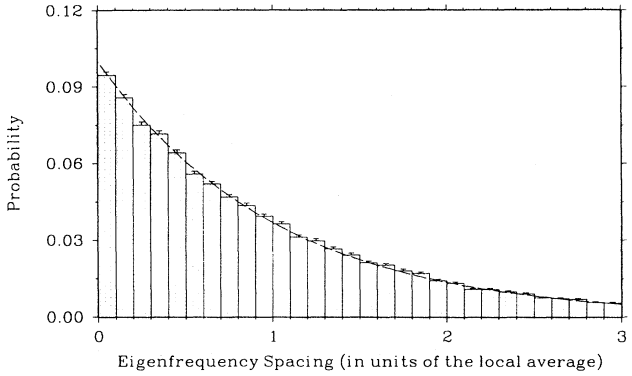

FIG. 11. Eigenfrequency spacing distribution for the first 46 959 eigenfrequencies of the cylindrical cavity specified in the text. The dashed line represents Poisson statistics.

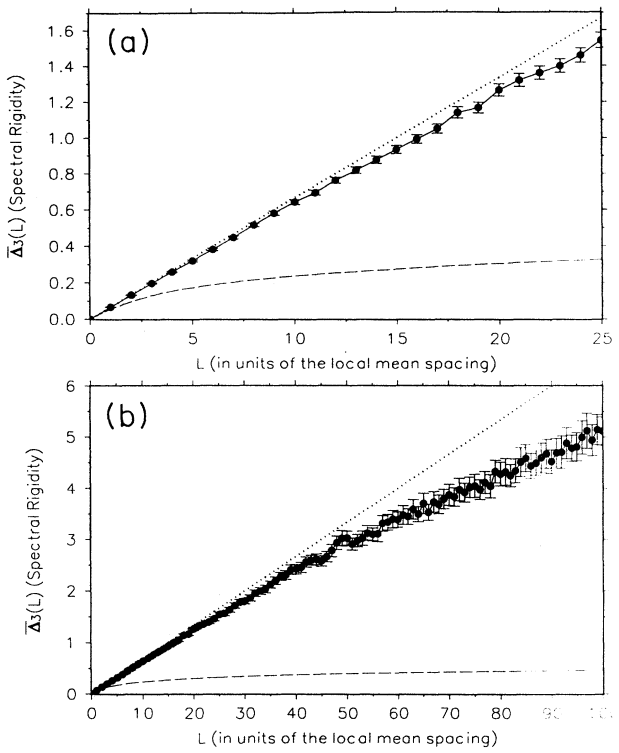

FIG. 12. Spectral rigidity for the first 5120 eigenfrequencies of the cylindrical cavity specified in the text. The dashed line is a theoretical GOE prediction, whereas the dotted line is $\bar{\Delta}_3(L)$ for the Poisson case.

modes because of the relation $J_0'(x) = -J_1(x)$; we get $\nu^{\mathrm{TE}}_{m=0,n,p} = \nu^{\mathrm{TM}}_{m=1,n,p}$, $n,p = 1,2,3,\ldots$.

We calculated the eigenfrequency spacing distribution and the spectral rigidity for TM and TE modes separately, as well as for mixed TM and TE modes. In these calculations, we treated all degeneracies as single resonances, i.e., we did not count zero spacings. The degeneracy-pruned calculations for pure TM and TE sequences of resonances as well as those for mixed TM and TE resonances showed good agreement with Poisson statistics. The results for the mixed TM-TE treatment are shown in Figs. 11 and 12. The nearest-neighbor spacing distribution, shown in Fig. 11, is approximated very well by the Poisson distribution. The spectral rigidity (see Fig. 12) shows good agreement with Poisson statistics up to an interval length of approximately 10; above there it increasingly deviates from the result for Poisson statistics.

We would expect Poisson statistics for a symmetrically shaped 2D microwave cavity due to the analogy with a quantum billard whose classical analogue has regular dynamics. We see here that a spatially symmetric 3D microwave cavity gives us the same statistical results as in a 2D cavity.

[1] M. C. Gutzwiller, *Chaos in Classical and Quantum Mechanics* (Springer-Verlag, New York, 1990), Chap. 16.

[2] M. L. Mehta, *Random Matrices*, 2nd ed. (Academic, New York, 1990).

[3] R. U. Haq, A. Pandey, and O. Bohigas, Phys. Rev. Lett. **48**, 1086 (1982); O. Bohigas, R. U. Haq, and A. Pandey, *ibid.* **54**, 1645 (1985).

[4] R. L. Weaver, J. Acoust. Soc. Am. **85**, 1005 (1989).

[5] D. Wintgen and H. Friedrich, Phys. Rev. Lett. **57**, 571 (1986).

[6] D. Delande and J. C. Gay, Phys. Rev. Lett. **57**, 2006 (1986).

[7] A. Holle, G. Wiebusch, J. Main, B. Hager, H. Rottke, and K. H. Welge, Phys. Rev. Lett. **56**, 2594 (1986); J. Main, G. Wiebusch, A. Holle, and K. H. Welge, *ibid.* **57**, 2789 (1986).

[8] B. D. Simons *et al.*, Phys. Rev. Lett. **71**, 2899 (1993).

[9] W. Jans *et al.*, J. Phys. A **26**, 3187 (1993).

[10] M. V. Berry and M. Robnik, J. Phys. A **17**, 2413 (1984).

[11] T. Prosen and M. Robnik, J. Phys. A **26**, 2371 (1993).

[12] G. R. Welch *et al.*, Phys. Rev. Lett. **62**, 893 (1989).

[13] A. Kudrolli *et al.*, Phys. Rev. E **49**, R11 (1994).

[14] S. Sridhar, Phys. Rev. Lett. **67**, 785 (1991).

[15] H.-J. Stöckmann and J. Stein, Phys. Rev. Lett. **64**, 2215 (1990).

[16] H.-D. Gräf *et al.*, Phys. Rev. Lett. **69**, 1296 (1992).

[17] M. Berry, in *Chaos and Quantum Physics*, edited by M. Giannoni, A. Voros, and J. Zinn-Justin (Elsevier, Amsterdam, 1991), pp. 251–304.

[18] J. V. Jose, in *New Directions in Chaos*, edited by Hao Bai-Lin (World Scientific, Singapore, 1990).

[19] In a related study, an experimental test of the theorem of isospectral domains was carried out [S. Sridhar and A. Kudrolli, Phys. Rev. Lett. **72**, 2175 (1994)].

[20] R. Balian and C. Bloch, Ann. Phys. (N.Y.) **84**, 559 (1974); Ann. Phys. (N.Y.) **64**, 271(E) (1971).

[21] R. Balian and C. Bloch, Ann. Phys. (N.Y.) **60**, 401 (1970).

[22] M. Born and E. Wolf, *Principles of Optics*, 5th ed. (Pergamon, Oxford, 1975), Sec. 3.1.1.
[23] A. J. Lichtenberg and M. A. Lieberman, *Regular and Stochastic Motion* (Springer-Verlag New York, 1983).
[24] R. P. Ratowsky, Ph.D. thesis, University of California at Berkeley, 1988 (unpublished).
[25] M. Bartsch *et al.*, Comput. Phys. Commun. **72**, 22 (1992).
[26] We investigated two prismlike cavities and one double-cone-like cavity, which we had solderd together of brass sheets, all in different stages of deformation. In addition, a commercially available toilet float ball made of copper and deformed by us was investigated.
[27] T. A. Brody, Lett. Nuovo Cimento **7**, 482 (1973).
[28] T. A. Brody *et al.*, Rev. Mod. Phys. **53**, 385 (1981).
[29] M. V. Berry and M. Tabor, Proc. R. Soc. London Ser. A **356**, 375 (1977).
[30] F. Haake, *Quantum Signatures of Chaos* (Springer, Berlin, 1991).
[31] M. V. Berry, Ann. Phys. (N.Y.) **131**, 163 (1981).
[32] T. Ishikawa and T. Yukawa, Phys. Rev. Lett. **54**, 1617 (1985).
[33] A. Shudo and Y. Shimizu, Phys. Rev. A **42**, 6264 (1990).
[34] O. Bohigas *et al.*, Phys. Rev. Lett. **52**, 1 (1984).
[35] T. Yukawa and T. Ishikawa, Progr. Theor. Phys. Suppl. **98**, 157 (1989).
[36] C. E. Porter, *Statistical Theory of Spectra* (Academic, New York, 1965).
[37] M. L. Mehta and J. Des Cloizeaux, Indian J. Math. **3**, 329 (1971).
[38] B. Dietz and F. Haake, Z. Phys. B **80**, 153 (1990).
[39] T. Prosen and M. Robnik, J. Phys. A **26**, 1105 (1993).
[40] F. J. Dyson and M. L. Mehta, J. Math. Phys. **4**, 701 (1963).
[41] H. Friedrich and D. Wintgen, Phys. Rep. **183**, 37 (1989).
[42] G. R. Welch, M. M. Kash, C.-h. Iu, L. Hsu, and D. Kleppner, Phys. Rev. Lett. **62**, 893 (1989).
[43] G. Wunner, Phys. Bl **45**, 139 (1989).
[44] Y. Chen *et al.*, J. Opt. Soc. Am. B **7**, 1805 (1990).

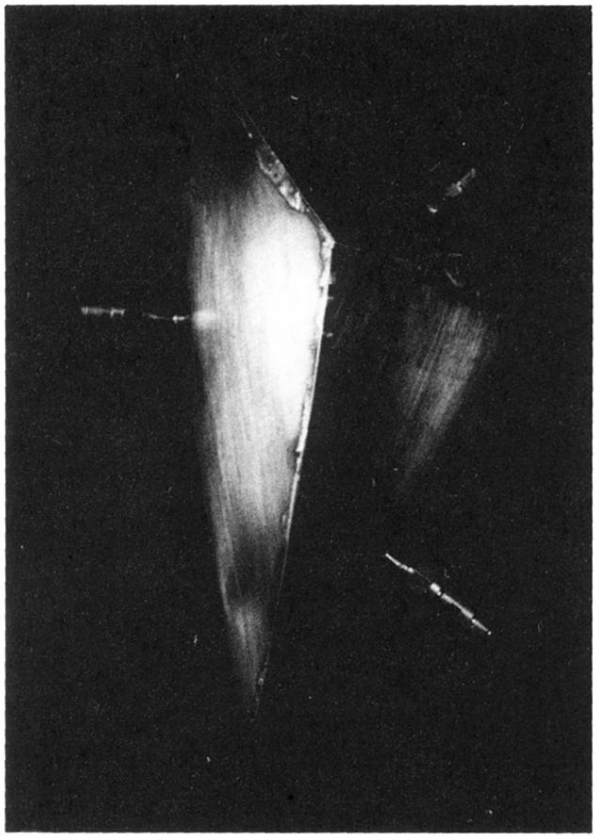

FIG. 5. Photograph of the cavity.